Biology and Medicine

Guano et al., Biol Med (Aligarh) 2016, 8:3
http://dx.doi.org/10.4172/0974-8369.1000283

Research Article Open Access

Zinc Oxide Crystals with Controlled Size and Morphology

Guano SE[1,3*], **Debut A**[2] **and Fernandez-Morales P**[3]

[1]*GIERIMP, Universidad Politécnica Salesiana, Quito, Ecuador*

[2]*CENCINAT, Universidad de las Fuerzas Armadas-ESPE, Quito, Ecuador*

[3]*Facultad de Ing. Industrial, Universidad Pontificia Bolivariana, Medellín, Colombia*

[*]**Corresponding author:** Guano SE, GIERIMP, Universidad Politécnica Salesiana, Quito, Ecuador, Tel: +59 (02) 3962900 Ext 2314; E-mail: sguano@ups.edu.ec

Received date: March 16, 2016; **Accepted date:** April 05, 2016; **Published date:** April 08, 2016

Abstract

Zinc Oxide (ZnO) has been synthesized by evaporation, condensation, and oxidation of metallic Zn under atmospheric pressure, the objective of this study is the growth the particles of ZnO and its relationship with the deposition zone. Pieces of Zn were introduced into a quartz tube acting as reactor which is placed inside the tube-furnace at 920-950°C under controlled pressure and heating profile. Carefully monitoring the temperature zones inside the reactor, ZnO crystals were growth. During heating, the oxygen in the surrounding environment reacted with the Zn pieces' surface to form a ZnO capsule with liquid and gaseous Zn inside. When the pressure inside the capsule surpasses the ambient pressure, cracks are formed in the oxide crust and the Zn vapor is released. Zinc in gaseous state oxidizes as it flows through air, and, depending on its trajectory, a variety of crystallites are obtained with size ranging from 20 nm, for the smallest particles, to 5 μm for the tetrapod nanostructures.

Keywords: Zinc oxide; Thermal oxidizing; Tetrapod

Introduction

Because of their interesting properties for electronic and light emission devices applications, the ZnO structures constitute an interesting topic of research [1,2]. In particular, the Zinc Oxide (ZnO) nanostructures with different shapes, such as wires [3,4], spheres [5–7] and belts [8,9], are useful for applications in nanophotonics [10]. The objective of this study is the growth the particles of ZnO and its relationship with the deposition zone.

ZnO can also be used in UV light emitters [11], spin functional devices, gas sensors [12], transparent electronics and surface acoustic wave devices [13]. The three most common methods for the synthesis of bulk ZnO crystals are hydrothermal [14,15], vapor phase [16–18], and growth from the melt state [19]. It has also been observed that the tetrapod contain legs of single crystals with hexagonal structure [3,10].

The Zinc Oxide generality grows with a wurtzita crystalline hexagonal structure [20-26]. The related lattice parameters are a=0.325 nm and c=0.512 [10,27,28]. The Zn atoms are tetrahedrally coordinate with four oxygens atoms [27–29], where the electrons of the d zinc layer hybridizes with the oxygen p layer, building the Zn-O alternating layers [13].

The ZnO particles synthetized were analyzed by means of X Ray Diffraction (XRD), Transmission Electron Microscopy (TEM), and Scanning Electron Microscopy (SEM). The XRD characterization indicated these particles have wurtzite structure and the optical properties have been studied with cathodeluminescence (CL). For TEM analysis a Tecnai G2 Spirit Twin instrument was used operated at 120 kV, mainly under diffraction contrast mode.

Material and Methods

The synthesis of ZnO is thermodynamically viable because its reaction has a large negative ΔG°, and the vapor pressure of Zn is about 1 atm at 900°C. The synthesis of ZnO is carried out for homogeneous reaction, gas-gas. In agreement with the Ellinghan diagram the growth of ZnO from Zn(g) and O_2(g) has favorable conditions when the furnace temperature is over 900°C. In such conditions, the production of Zn(g) is higher and there will be more molecules for reacting with O_2, and the reaction occurred in few minutes after beginning.

In this work, it is reported a synthesis of ZnO in a furnace tube in static air conditions. Zinc pieces with a size of 3-8 mm (99.98% purity, Pb 0.01%, Fe 0.01%. As 0.01 ppm) where placed in an alumina boat located in a quartz tube with a diameter of 5 cm. The two ends of the tube were open during the growth process. Then, the horizontal tube furnace was heated from 250°C up to 940°C using a rate of 10°C/min, maintaining the work temperature for 15 minutes, and then cooled down to room temperature whit a ramp of 120°C/h. This experimental procedure is similar to the procedure reported in Ronning et al. [10]. However, authors of that research work growth ZnO on Si (100) and set up an alumina tube with a diameter of 5cm with one side of the tube sealed and the other opened along through the growth process. These factors determine differences in a reaction temperature and deposition temperature zones.

During the heating process a ZnO layer forms on the surface of the original Zn particles, creating a crust or capsule that separates liquid Zn and the surrounding air. When the internal pressure of the capsule is larger than the pressure in the chamber, some cracks are produced in the crust, and Zn(g) is liberated. The Zn(g) reacts with O_2 while it is transported towards the end of the alumina tube, where it is deposited in regions under different temperatures. Abduev et al. [30], reported the chamber formation and the cracks presence when the system exceeds 920°C, obtaining white fluffy and bulk products.

The structural analysis of the ZnO particles was performed by means of XRD using Cu-Kα 1.54184 Å radiation. The optical properties of the ZnO particles were studied and analyzed by CL measurements in a SEM equipped with a CL detector with spatial resolution. The CL analysis was performed at room temperature. The electron beam voltage was kept constant at 4.5 kV throughout the whole experiment.

Results

The ZnO deposited on the ends of tube has a tetrapod-like homogeneous morphology. This structure is present in all the experiments. The Figure 1 shows a relation between deposition zone and the ZnO morphologies. There were also observed tetrapods and whiskers out of the furnace on the alumina rod, on the reactor wall and plates. In addition, it was observed dendritic structures on the furnace center.

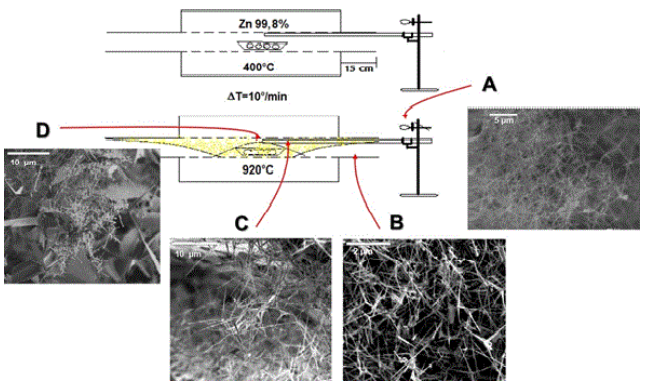

Figure 1: SEM -SE images of ZnO synthesized at 920°C. A. ZnO particles deposited out of furnace it observe whiskers, B. Particles deposited on the wall reactor can see wires and tetrapod, C. Particles deposited on the alumina rod inside the furnace in can observe tetrapods, D. ZnO deposited in the center of furnace present plates, wires, dendritic structures.

The high purity of ZnO synthesized by this method, in agreement with the spectrum of the wurtzite structure and the absence the impurity peaks, indicates that the Zinc Oxide have a well-defined crystalline structure [16,31].

Figures 2 and 3 show the SEM and TEM images. At low magnification it can be clearly observed multiple-twined on the core. The diameter of the tetrapods' legs decreases from the center up to de tip. The same results were reported by Ye Zhang et al. [31]. Figures 2A and 2B show some tetrapods whose legs' length are around 2 um and 750 nm. Figure 3 shows a tetrapod with legs of approximately 1 um of length.

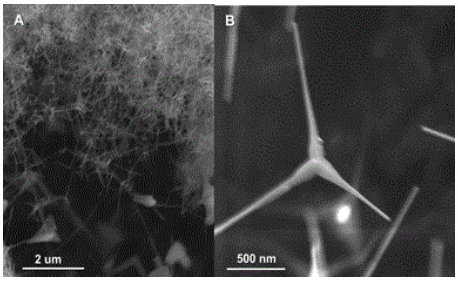

Figure 2: SEM-SE imagens composition ZnO particles synthetized at 920°C and collected out of the center of reactor, A. a cluster of tetrapods, B. Image SEM-SE High resolution of tetrapod show legs of 1um of length.

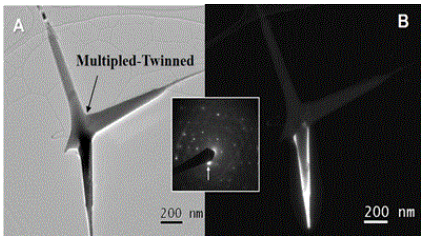

Figure 3: TEM Images composition of ZnO particles synthetized. A. TEM multi-beam image of tetrapods, B centered-dark-field images of individual nanorod belonging to the tetrapods (leg) it insert the corresponding selected area diffraction pattern; the arrow indicated the reflection responsible for the image.

In Figure 4A it can be observed that the length of the tetrapods legs is in the order of 1.5 to 3 um. In Figure 4B it can be seen the CL qualitative characterization image at room temperature. This results is in agreement with results obtained by Roy et al. [32]. The intensity contrast in the legs is due to the incidence angle between the surface and the electron beam.

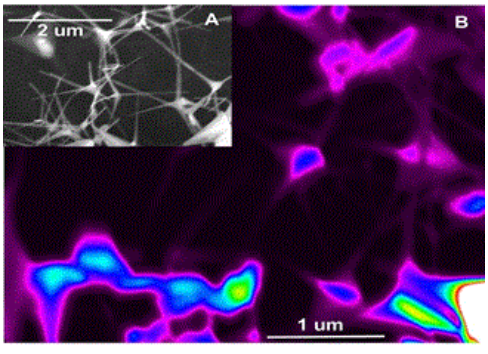

Figure 4: SEM–CL images composition of ZnO Tetrapods. A SEM-SE image show tetrapods and whiskers, B. SEM-CL image show magnification of A can observe the qualitative CL emission.

Discussion

Synthesis: This experiment is interesting because: (a) A very close to thermodynamics equilibrium, with little or no temperature gradient. It can be affirmed because the synthetized particles have no defects in these crystalline structure. It is evidenced in the symmetry of the particles observed in Figure 2 and in the fact that the tetrapod's legs are a monocrystal as confirmed in Figure 3. (b) The evaporation occurs in an oxygen deficient region. Therefore, the ZnO crystals are deposited at the ends of tube and the reaction forms a tetrahedron core. This is related with the luminescence properties of ZnO particles and with the oxygen superficial vacancies [33]. The tetrahedron core formation is reported on some recent investigations [10]. Based on the results obtained in this research work we can affirm that if the core is deposited at the ends of reactor, it grows as tetrapods-like structure. Instead, if the core stays around the reactors' center, it can observe the formation of nanostructured particles, as shown in Figure 1. (c) The crystals that grew on the synthetization process have high quality crystallite, and little defects. Figure 3B confirms that every tetrapod leg is a monocrystal. Such effect can be seen in the selected area diffraction pattern (SDAP) on Figure 3 that showing the electron beam that form the dark field image.

Optical properties: The ZnO particles synthesized presented a CL emission, it is intense in bulk of particles and decreases on the surface, also is less intense at the wires.

Conclusions

The ZnO synthesized by simple evaporation and direct oxidation of Zinc with ambient air grows in different shapes, but reports the presence of tetrapods in all runs. The length of legs varies from 0.75 to 20 um for different particles, while the diameter varies from 0.2 to 2 um. The crystal shapes produced have hexagonal, wires, plates and tetrapod morphologies in all runs. The shape of the nanostructure depends on the deposition zone.

References

1. Choi S, Berhane AM, Gentle A, Ton-That C, Phillips MR, et al. (2015) Electroluminescence from localized defects in zinc oxide: toward electrically driven single photon sources at room temperature. ACS Appl Mater Interfaces 7: 5619-5623.
2. Chong SK, Dee CF, Abdul Rahman S (2013) Structural and photoluminescence studies on catalytic growth of silicon/zinc oxide heterostructure nanowires. Nanoscale Res Lett 8: 174.
3. Ye N, Chen CC (2012) Investigation of ZnO nanorods synthesized by a solvothermal method, using Al-doped ZnO seed films. Opt Mater (Amst) 34: 753–756.
4. Nayeri FD, Soleimani EA, Salehi F (2013) Synthesis and characterization of ZnO nanowires grown on different seed layers: The application for dye-sensitized solar cells. Renew Energy 60: 246–255.
5. Li Q, Wang E, Siheng L, Wang C, Tian C, et al. (2009) Template-free polyoxometalate-assisted synthesis for ZnO hollow spheres. J Solid State Chem 182: 1149–1155.
6. Wei Y, Huang Y, Wu J, Wang M, Guo C, et al. (2013) Synthesis of hierarchically structured ZnO spheres by facile methods and their photocatalytic deNOx properties. J Hazard Mater 248-249: 202-10.
7. Pandey P, Kurchania R, Haque FZ (2015) Controlled hydrothermal synthesis, structural and optical analysis of nanometer-sized ZnO spheres. Opt - Int J Light Electron Opt 126: 301–303.
8. Leung YH, Djurisic AB, Gao J, Xie MH, Wei ZF, et al. (2004) Zinc oxide ribbon and comb structures: Synthesis and optical properties. Chem Phys Lett 394: 452–457.
9. Liao L, Liu DH, Lia JC, Liu C, Fu Q, et al. (2005) Synthesis and Raman analysis of 1D-ZnO nanostructure via vapor phase growth. Appl Surf Sci 240: 175–179.
10. Ronning C, Shang NG, Gerhards I, Hofsass H, Seibt M (2005) Nucleation mechanism of the seed of tetrapod ZnO nanostructures. J Appl Phys 98: 034307.
11. Aoki T, Hatanaka Y, Look DC (2000) ZnO diode fabricated by excimer-laser doping. Appl Phys Lett 76: 3257.
12. Katsarakis N, Bender M, Cimalla V, Gagaoudakis E, Kiriakidis G (2003) Ozone sensing properties of DC-sputtered, c-axis oriented ZnO films at room temperature. Sensors Actuators B Chem 96: 76–81.
13. Pearton SJ, Norton DP, Ip K, Heo YW, Steiner T (2005) Recent progress in processing and properties of ZnO. Prog Mater Sci 50: 293–340.
14. Kale RB, Lu SY (2013) Hydrothermal growth and characterizations of dandelion-like ZnO nanostructures. J Alloys Compd 579: 444–449.
15. Liu C, Li H, Jie W, Zhang X, Yu D (2006) Preparation of ZnO cluster and rod-like whiskers through hydrothermal methods. Mater Lett 60: 1394–1398.
16. Fischer AM, Srinivasan S, Garcia R, Ponce FA, Guaño SE, et al. (2007) Optical properties of highly luminescent zinc oxide tetrapod powders. Appl Phys Lett 91: 121905.
17. Chen YX, Lewis M, Zhou WL (2005) Zno nanostructures fabricated through a double-tube vapor-phase transport synthesis. J Cryst Growth 282: 85–93.
18. Vanheusden K, Seager CH, Warren WL, Tallant DR, Voigt JA (1996) Correlation between photoluminescence and oxygen vacancies in ZnO phosphors. Appl Phys Lett 68: 403–405.
19. Ozgur U, Alivov YI, Liu C, Teke A, Reshchikov M, et al. (2005) A comprehensive review of ZnO materials and devices. J Appl Phys 98: 041301.
20. Dal Corso A, Posternak M, Resta R, Baldereschi A (1994) Ab initio study of piezoelectricity and spontaneous polarization in ZnO. Phys Rev B Condens Matter 50: 10715-10721.
21. Mangamma G, Bakyalakshmi V, Kamruddin M, Dash S, Tyagi AK (2013) Formation of Nanorods of Undoped and Doped ZnO. IEEE Trans Nanotechnol 12: 919–924.
22. Maleki Shahraki M, Shojaee SA, Faghihi Sani MA, Nemati A, Safaee I (2011) Two-step sintering of ZnO varistors. Solid State Ionics 190: 99–105.
23. Gonzalez-Rolon B, Ireta-Moreno F (2011) Desarrollo y producción de varistores de ZnO dopados para media tensión 13 000 V a 34 000 V. Ing Investig y Tecnol XII: 149–155.
24. Willander M, Nur O, Zhao QX, Yang LL, Lorenz M, et al. (2009) Zinc oxide nanorod based photonic devices: recent progress in growth, light emitting diodes and lasers. Nanotechnology 20: 332001.
25. Elumalai NK, Jin TM, Chellappan V, Jose R, Palaniswamy SK, et al. (2013) Electrospun ZnO Nanowire Plantations in the Electron Transport Layer for High-Efficiency Inverted Organic Solar Cells. Appl Mater interfaces 5: 9396–9404.
26. Shokry Hassan H, Kashyout AB, Morsi I, Nasser AAA, Ali I (2014) Synthesis, characterization and fabrication of gas sensor devices using ZnO and ZnO:In nanomaterials. Beni-Suef Univ J Basic Appl Sci 3: 216–221.
27. Chen ZG, Anze N, Feng L, Hongtao C, Hui-Ming C, et al. (2007) Synthesis and photoluminescence of tetrapod ZnO nanostructures. Chem Phys Lett 434: 301–305.
28. Chevalier-César C, Capochichi-Gnambodoe M, Leprince-Wang Y (2014) Growth mechanism studies of ZnO nanowire arrays via hydrothermal method. Appl Phys A 115: 953–960.
29. Hongsith N, Chairuangsri T, Phaechamud T, Choopun S (2009) Growth kinetic and characterization of tetrapod ZnO nanostructures. Solid State Commun 149: 1184–1187.
30. Abduev AK, Asvarov AS, Akhmedov AK, Baryshnikov VG, Terukov EI (2002) Vapor phase synthesis of ZnO structures. Tech Phys Lett 28: 952–954.

31. Dai Y, Zhang Y, Li QK, Nan CW (2002) Synthesis and optical properties of tetrapod-like zinc oxide nanorods. Chem Phys Lett 358: 83–86.

32. Roy VL, Djurisic AB, Chan WK, Gao J, Lui HF, et al. (2003) Luminescent and structural properties of ZnO nanorods prepared under different conditions. Appl Phys Lett 83: 141.

33. Meyer BK, Alves H, Hofmann DM, Kriegseis W, Forster D, et al. (2004) Bound exciton and donor – acceptor pair recombinations in ZnO. Phys Stat Sol 260: 231–260.

This article was originally published in a special issue, entitled: **"Recent Advances in Biology & Nanotechnology"**, Edited by Saurabh RamBihariLal Shrivastava